Current Research in Food Science 5 (2022) 1944–1954

Contents lists available at ScienceDirect

Current Research in Food Science

journal homepage: www.sciencedirect.com/journal/current-research-in-food-science

Green extraction, chemical composition, and *in vitro* antioxidant activity of theabrownins from Kangzhuan dark tea

Yi Liu [a,b], Hong-Yan Liu [a], Xiao Yang [a], Fan Zhu [c], Ding-Tao Wu [d], Hua-Bin Li [e], Ren-You Gan [a,*,1]

[a] Research Center for Plants and Human Health, Institute of Urban Agriculture, Chinese Academy of Agricultural Sciences, Chengdu National Agricultural Science & Technology Center, Chengdu, 610213, China
[b] University of Vigo, Nutrition and Bromatology Group, Department of Analytical Chemistry and Food Science, Faculty of Science, E32004, Ourense, Spain
[c] School of Chemical Sciences, University of Auckland, Private Bag 92019, Auckland, 1142, New Zealand
[d] Key Laboratory of Coarse Cereal Processing (Ministry of Agriculture and Rural Affairs), Sichuan Engineering & Technology Research Center of Coarse Cereal Industralization, School of Food and Biological Engineering, Chengdu University, Chengdu, 610106, China
[e] Guangdong Provincial Key Laboratory of Food, Nutrition and Health, Department of Nutrition, School of Public Health, Sun Yat-Sen University, Guangzhou, 510080, China

ARTICLE INFO

Keywords:
Tibetan tea
Theabrownins
Ultrasonic-assisted extraction
Deep eutectic solvents
LC-MS/MS
In vitro antioxidant activity

ABSTRACT

Theabrownins (TBs) in dark tea have received increasing attention for their multiple health benefits. In this study, ultrasound assisted extraction with deep eutectic solvent (UAE-DES) was developed for the extraction of TBs from Kangzhuan dark tea (KZDT). The highest yield (12.59%) of TBs was obtained using UAE-choline (ChCl)/malic acid (MA) with a liquid to solid ratio of 20:1 (v/w), ultrasonic power of 577 W, ultrasonic time of 25 min, and water content of 30%. TBs were further eluded by silica gel to obtain six theabrownine fractions (TBFs), namely, TBFs1, TBFs2, TBFs3, TBFs4, TBFs5, and TBFs6. LC-MS/MS revealed that flavonoids, terpenes, phenolic acids, alkaloids, lipids, and amino acids are the leading components of TBFs. The TBFs4, with the DPPH, ABTS, and FRAP values of 45.08 ± 0.42 μM Ascorbic acid/g DW, 178.52 ± 0.29 μM Trolox/g DW, and 370.85 ± 6.00 μM Fe(II)/g DW, respectively, showed the highest antioxidant activity among all the TBFs. Overall, this study first provided the evidence that UAE-ChCl/MA combining with silica gel was effective to extract TBs from KZDT, and the 6,7-dihydroxycoumarin-6-glucoside and neohesperidin were found as the leading compounds in the TBFs, providing a guidance for the chemical research and further utilization of dark tea and its TBs.

1. Introduction

Chinese dark tea is mainly classified into Kangzhuan dark tea (KZDT), Liubao tea, Fubrick tea, Pu-erh tea, and Qingzhuan tea according to their manufacturing procedures and source of raw materials (Lin et al., 2021; Liu Y.T. et al., 2022). Among above tea, KZDT is also known as "Ya'an Tibetan tea" from China's Sichuan Province (Zheng et al., 2020; Zheng et al., 2021; Liu Y.T. et al., 2022). The processing procedures of tea influence its phytochemical compositions and bioactivities (Ding et al., 2022).The manufacturing procedures of KZDT include withering, rolling, piling, brick-pressing, drying, and storage (Xie et al., 2018). Theabrownins (TBs), one of the most active and abundant pigments found in dark tea, have the highest water solubility (Liu Y.T. et al., 2022). They are considered superior to theaflavins (TFs) or thearubigins (TRs) in physicochemical and medicinal properties (Jin et al., 2018; Chen et al., 2022). The health-promoting benefits of TBs, such as antioxidation, anticancer (Chen et al., 2022), anti-inflammatory, and hypolipidemic activities (Ma et al., 2022), have been reported, but the development and utilization of them are insufficient. The chemical composition of TBs directly determines their bioactivities. TBs are a family of macromolecules transformed from a complex of heterogeneous components, namely, polyphenols, caffeine, proteins, carbohydrates, and amino acids, but only a handful of studies described their chemical makeup (Kuang et al., 2020; Chen et al., 2022). Therefore, it is of great importance to clarify the chemical composition of TBs from KZDT.

Organic solvents (i.e., ethanol, chloroform, methanol, and ethyl acetate) are mainly used to extract TBs in dark tea (Zou et al., 2016; Huang et al., 2019). The organic solvents exhibit many drawbacks, such as environmentally unfriendly, and hard to degrade (Liu et al., 2022a). So,

* Corresponding author.
E-mail address: ganrenyou@163.com (R.-Y. Gan).
[1] Current address: Singapore Institute of Food and Biotechnology Innovation (SIFBI), Agency for Science, Technology and Research (A*STAR), Singapore 138669, Singapore.

https://doi.org/10.1016/j.crfs.2022.10.019
Received 14 July 2022; Received in revised form 29 August 2022; Accepted 14 October 2022
Available online 17 October 2022

Abbreviations

KZDT	Kangzhuan dark tea
TBs	theabrownins
TBFs	theabrownine fractions
ChCl	choline chloride
MA	malic acid
UAE-DES	ultrasound assisted extraction with deep eutectic solvent
RSM	response surface methodology
Gly	glycerol
EG	ethylene glycol
Suc	sucrose
Xyl	xylitol
CA	citric acid
MA	malic acid

it is needful to develop green and effective extraction technologies to obtain TBs from KZDT. Compared to organic solvents, deep eutectic solvents (DES) possess some obvious advantages such as easy preparation, stability, low cost, and safety, which fully follow the rules of green extraction (Cai et al., 2019). Choline chloride (ChCl) is a widely used hydrogen bond acceptor (HBA), and ChCl-DES has been applied in the extraction of bioactive compounds from plants, such as *Cannabis sativa* (Liu et al., 2022b) and green tea (*Camellia sinensis*) (Luo et al., 2020). The ultrasound assisted extraction with DES (UAE-DES) can enhance the yield of bioactive compounds via acoustic cavitation (Wang et al., 2021). This process follows another rules of green extraction, that is, to degrade energy consumption using innovative technologies (Luo et al., 2020). Thus, UAE-DES combined with silica gel is speculated as an effective method to extract TBs from KZDT, and theabrownine fractions (TBFs) eluded by silica gel from TBs have different chemical composition and antioxidant activities.

To test this hypothesis, this study firstly extracted TBs from KZDT by DES-UAE. TBs were further fractionated by silica gel to obtain six TBFs. The antioxidant activity of TBFs was assessed by DPPH free radical scavenging, ABTS free radical scavenging, and FRAP assays. In addition, the chemical composition of TBFs was identified by LC-MS/MS analysis. This study provided scientific insight into the chemical components of TFBs eluded by silica gel from TBs, which could help understand their health functions and promote their application.

2. Materials and methods

2.1. Chemicals and reagents

Glycerol (Gly) , ethylene glycol (EG), sucrose (Suc), xylitol (Xyl), citric acid (CA), malic acid (MA), and gallic acid were bought from Macklin Biochemical Co., Ltd., Shanghai, China. Silica powder, Folin–Ciocalteu's phenol, 2,2-diphenyl-1-picrylhydrazyl (DPPH) 2,4,6-tri(2-pyridyl)-S-triazine (TPTZ), and 2,2′-azino-bis (3-ethylbenz-thiazoline-6-sulfonic acid) (ABTS) were purchased from Yishan Huitong Technology Co., Ltd., Beijing, China. Analytical-grade or chromatographic-grade methanol, formic acid, acetonitrile, hydrochloric acid, and ethanol were bought from Kelon Chemical Reagent Factory, Chengdu, China. Deionized water was made from a water purification system, ELGA, China.

2.2. Preparation of sample

Kangzhuan tea (KZDT) was purchased from Sichuan Kangrun Tea Co., Ltd. (Ya'an, China). The tea was run into powders using a pulverizer. The final powders were stored at 4 °C for two weeks.

2.3. Preparation of DES

DES was synthesized based on our prior study (Luo et al., 2020). The ChCl/hydrogen bond donors (ChCl/HBD), abbreviations of the prepared DES solutions, and ChCl/HBD molar ratios were listed in Table S1. Briefly, the molar ratio of ChCl/HBD of DES was mixed at 1:2. Deionized water of 20% (m/V) was added with gentle stirring and heated at 80 °C until uniform DES solutions were obtained. DES solutions were cooled down and stored at 4 °C.

2.4. Extraction of KZDT

2.4.1. UAE-DES

KZDT powder was extracted by UAE-DES according to our prior study (Luo et al., 2020). Briefly, KZDT powder (1.0 g) was added into a 100 mL glass beaker, and then added 30 mL DES solutions to mix. The UAE was carried out using a XH-300UP Multifunctional extractor (Beijing, China), and the UAE-DES extraction conditions were the liquid to solid ratio at 10:1–50:1, the ultrasonic power at 330–850 W, the ultrasonic time at 2–34 min, and the water content in ChCl/MA at 10%–50%. In the course of the extraction, samples were always kept in ice water to avoid the degrading of TBs. The supernatant was collected after the extracts were centrifuged using a 5424R Eppendorf centrifuge (Shanghai, China) at 12000×*g* for 5 min.

2.4.2. UAE with ethanol extraction

KZDT powder was extracted by UAE with ethanol depending on a precedent study (Liu et al., 2021). Briefly, KZDT powder (1.0 g) admixed with anhydrous ethanol (20 mL). The extraction process was then acted at ultrasonic power of 577 W for 25 min. In the course of the extraction, the sample was always kept in ice water. The supernatant was collected after the extracts were centrifuged using a 5424R Eppendorf centrifuge (Shanghai, China) at 12000×*g* for 5 min.

2.4.3. DES-maceration extraction (ME)

KZDT powder was extracted by ME as described previously (Liu et al., 2021). Briefly, KZDT powder (1.0 g) was admixed with 30% ChCl/MA aqueous solution (20 mL). The extraction was then acted in a shaking water bath at 25 °C for 24 h. The supernatant was collected after the extracts were centrifuged using a 5424R Eppendorf centrifuge (Shanghai, China) at 12000×*g* for 5 min.

2.5. Optimization of UAE-DES

Initially, TBs were extracted by UAE-DES, and the effects of five factors, including liquid to solid ratio (10:1–50:1 mL/g), ultrasonic power (330–850 W), ultrasonic time (2–34 min), and water content in ChCl/MA (10–50%) were researched by a single-factor experiment based on our previous study (Luo et al., 2020). Response surface methodology (RSM) with a four-level-three-factor Box-Behnken Design (BBD) was used to optimize the extraction parameters, like liquid to solid ratio (X_1), ultrasonic power (X_2), ultrasonic time (X_3), and water content in ChCl/MA (X_4,), to obtain the highest TBs. According to the single-factor-experiment results, the actual levels and coded of 4 parameters in the extraction process are shown in Table S2. The analysis of variance (ANOVA) was used to determine significant differences among the treatments. 3D-surface plots were applied to observe the interactive effects of the significant variables on the TBs yields.

2.6. Preparation of TBs from KZDT

TBs from KZDT were prepared as described previously (Wu et al., 2020). After the extraction of KZDT under the optimal conditions of UAE-DES, the extracts were collected and mixed, filtered, and concentrated. The above concentrated solution was extracted by the ethyl acetate for 3 times successively. The aqueous phases were collected and

poured into a conical flask, and anhydrous ethanol was slowly added to make the volume fraction of ethanol 80% before standing for 8 h. Centrifugation was performed at 4200 ×g for 20 min to collect the precipitates, which were TBs in KZDT. The TBs were fully dissolved with distilled water before freeze-drying. The lyophilized TBs powder was collected and stored at 4 °C for next use.

2.7. Quantification of theabrownins (TBs)

The content of TBs was measured using a system approach as previously described (Wang et al., 2018). TBs solution was prepared by dissolving TBs (0.1 g) in distilled water (20 mL). TBs solution/KZDT extracts (25 mL) and 25 mL n-butanol were mixed into a funnel and shaken for 3min. After stratification, 2 mL sample of the aqueous phases was mixed with 2 mL of saturated oxalic acid solution, 6 mL of distilled water, and 15 mL 95% ethanol (solution B) to 25 mL. The E_B of solution B was measured with a UV-5500 spectrophotometer (Metash Instruments Co., Ltd., Shanghai, China) at 380 nm. The TBs yield (%) was calculated as the following:

$$TBs\ (\%) = \frac{7.06 \times 2 \times E_B}{dried\ weight\ (\%)} \times 100\%$$

where E_B is the corresponding spectrophotometer reading of all the samples. Dried weight is the weight of a sample without water.

2.8. Preparation of theabrownine fractions (TBFs)

Based on a previous method, TBs from KZDT were dispersed by using silica gel as the stationary phase and methanol aqueous solution as the mobile phase (Xie et al., 2019). First, the 100–200 mesh silica gel powder was washed with distilled water to neutral pH before drying at 110 °C for 24 h. It was required to be activated at 100 °C for 2–3 h before the experiment. The pre-treated silica gel powder (500 g) was sequentially slurry-packed in a 60.6 mm × 218.5 mm column with the methanol, and 2–3 volume of methanol was used for equilibration. The TBs (50 mg/mL) were then loaded onto this column. Preparation of theabrownine fractions (TBFs) was carried out by sequentially eluting with 100% methanol (0–20 min), 100−80% methanol (21–40 min), 80−60% methanol (41–60 min), 60−40% methanol (61–80 min), 40−20% methanol (81–100 min), and 20−0% methanol (101–120 min) with a flow of 20 mL/min. Six TBFs were collected, namely, TBFs1 (100% methanol), TBFs2 (100−80% methanol), TBFs3 (80−60% methanol), TBFs4 (60−40% methanol), TBFs5 (40−20% methanol), and TBFs6 (20−0% methanol). TBFs were rotary-evaporated at 50 °C, and then stored at 4 °C for further identification and antioxidant activity assay.

2.9. LC-MS/MS analysis of TBFs

The chemical components in TBFs were detected by LC-MS/MS based on our precedent study (Mai et al., 2022). It was separated on a LC System (Thermo Scientific, San Jose, USA) with a Hypersil GOld C18 column (2.1 × 100 mm, 1.9 μm). The mobile phase consisted of solvent A (0.1% formic acid aqueous solution) and solvent B (acetonitrile). The column was eluted at a flow rate of 0.3 mL/min with a gradient of 1% solvent B (0–4 min), 1–10% solvent B (4–15 min), 10–15% solvent B (15–25 min), 15–25% solvent B (25–30 min), 25–40% solvent B (30–35 min), 40–80% solvent B (35–45 min), and 80–100% solvent B (45–50 min). The injection volume is 5 μL, and column temperature is 30 °C. ESI−MS (orbitrap) analysis was performed in the m/z range of 100–1000, and the enhanced product ion (EPI) scan was performed to identify their fragment ions. The ion source parameters were capillary voltage with −12V, spray voltage with 4.5 kV, resolution at 70,000, and heated capillary temperature at 275 °C. The chemical components were analyzed by comparing the parent and fragment ions with the MassBank database (https://massbank.eu/MassBank/).

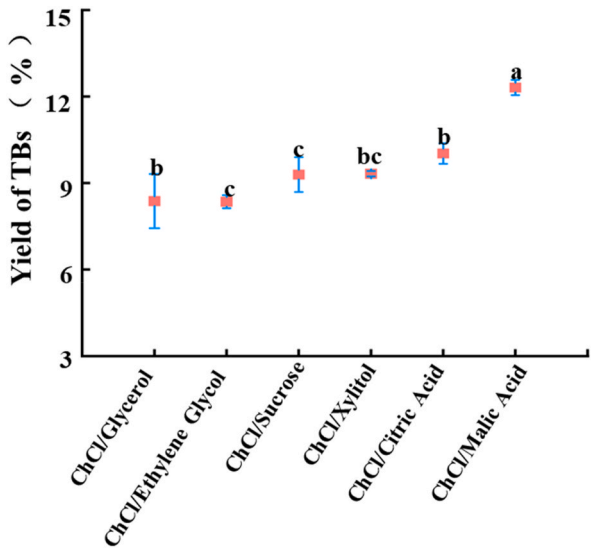

Fig. 1. Theabrownins (TBs) yields of the Kangzhuan dark tea extracts based on 6 selected DESs. Data are expressed as means ± SD (n = 3). Values with superscript letters (a–c) are significantly different across columns ($P < 0.05$).

2.10. Determination of antioxidant capacity in vitro

2.10.1. DPPH radical scavenging activity

The DPPH antioxidant activity of TBFs was determined based on a prior study with a minor modification (Liu et al., 2021; Zou et al., 2021; Zhu et al., 2021; Ding et al., 2022). The DPPH methanol solution (0.05 mg/mL) was adjusted with methanol to reach an absorbance of 0.789 ± 0.02 at 517 nm. 100 μL of sample solutions was mixed with 1.9 mL of the DPPH working solution at room temperature for 10 min in the dark. Then the spectrophotometer reading at 517 nm of the mixture was determined. The results were calculated using a calibration curve of ascorbic acid (5–50 μM) and expressed as μM Ascorbic acid/g dry weight (DW) of TBs.

2.10.2. ABTS radical scavenging activity

The ABTS capacity of TBFs was determined based on our prior study with a minor modification (Mai et al., 2022). The $ABTS^{\bullet+}$ solution (7 mM) was mixed with potassium persulfate solution (2.45 mM) (1:1, *v/v*) and incubated for 17 h in the dark to prepare the $ABTS^{\bullet+}$ stock solution. The $ABTS^{\bullet+}$ stock solution was adjusted with deionized water to reach an absorbance of 0.758 ± 0.03 at 734 nm. 100 μL of sample solutions were mixed with 1.9 mL of $ABTS^{\bullet+}$ working solution at room temperature for 6 min in the dark, then the absorbance of the mixture at 734 nm was measured. The standard curve was carried out with standard Trolox solution (50–800 μM), and the results were expressed as μM Trolox/g dry weight (DW) of TBs.

2.10.3. FRAP assay

The FRAP capacity of TBFs was determined based on our prior study with a minor modification (Gan et al., 2017). The FRAP working solution was prepared by incubating 10 mM TPTZ solution with 20 mM ferric chloride solution in 300 mM sodium acetate buffer at a volume ratio of 10:1:1 (*v/v/v*). 100 μL of sample solutions was mixed with 1.9 mL of the FRAP working solution for 4 min at room temperature. Then the absorbance of the mixture at 593 nm was measured. The ferrous sulfate (20–1000 μM) was applied to make a standard curve, and the results were shown as μM Fe(II)/g DW of TBs.

2.11. Statistical analysis

The data among treatments were compared by the ANOVA with *post*

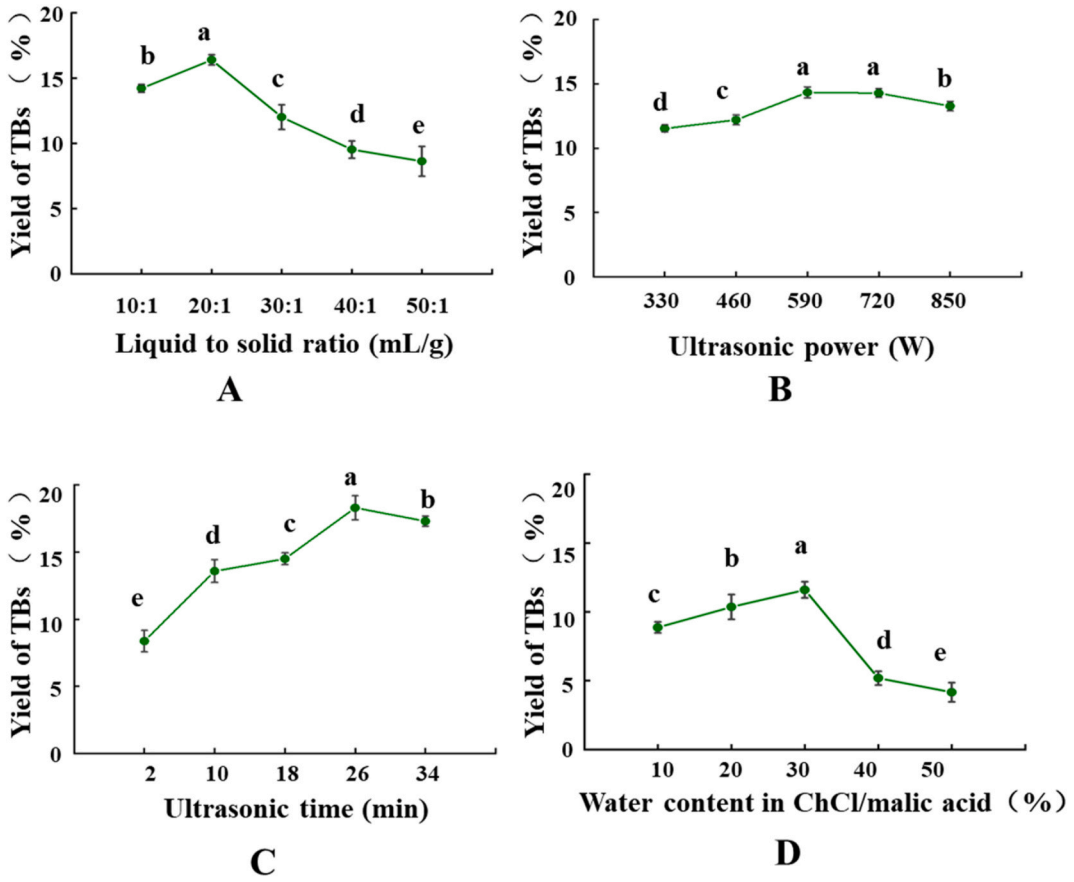

Fig. 2. Single-factor experimental design in measuring the effect of each factor on the yield of TBs. (A) Liquid to solid ratio (mL/g), (B) ultrasonic power (w), (C) ultrasonic time (min), and (D) water content in ChCl/MA (%).Values with superscript letters (a–e) are significantly different across columns ($P < 0.05$).

hoc Least Significant Difference (LSD) and Duncan's tests in SPSS 20.0 software (IBM Corp., Armonk, NY, USA) and displayed as means ± standard deviation. The data among treatments were tested for normality (Kolmogorov-Smirnov test) prior to ANOVA. The RSM response graphs were plotted using Design-Expert 13 (Stat-Ease, Inc., Minneapolis, USA) software. LC-MS/MS dates were acquisition using Xcalibur 4.0 software and Compound Discoverer 3.3 software (Thermo Scientific, San Jose, USA). $P < 0.05$ was defined as statistically significant.

3. Results and discussion

3.1. Selection of DES

DES is emergent solvent with high extraction rate of phytochemicals. The screening of different DES is the foremost work that should be done for TBs extraction from KZDT. In Fig. 1, the prepared ChCl-based DES, including ChCl/MA, ChCl/Gly, ChCl/Suc, ChCl/Xyl, ChCl/EG, and ChCl/CA, were further tested. It was significant that the yield of TBs in the ChCl/MA was the highest. A prior study reported that the ChCl/MA presented a high protective effect against the thermal degradation of extracts, which was mainly related to the low pH value of the DES and the molecular interactions (Benvenutti et al., 2022). Thus, ChCl/MA was selected as the DES for TBs extraction for further study.

3.2. Extraction optimization of TBs using UAE-DES

3.2.1. Single-factor experiments results

There has been no research to optimize the fermentation parameters that affect the yield of TBs in KZDT using single-factor experiments and RSM. The impacting factors for TBs content in UAE−DES, including solid to liquid ratio, water content in ChCl/MA, ultrasonic power, and ultrasonic time, were studied though single-factor experiment.

As the liquid to solid ratio (Fig. 2A), the TBs yield elevated as the liquid to solid ratio elevated from 10: 1 to 20:1 mL/g, but then the TBs yield dropped, as the liquid to solid ratio was further raised from 20:1 mL/g. The decreasing trend of TBs yield after the point "20:1 mL/g" may be explained as the volume of the DES increased, the dissolution of TBs was inhibited by other components of tea, which was not conducive to extraction (Durak and Gawlik-Dziki, 2014). So, the most fitted liquid to solid ratio range from 10:1 to 30:1 mL/g was recommended for the highest TBs. For the ultrasonic power (Fig. 2B), the TBs yield elevated as the ultrasonic power heightened from 330 to 720 W, but the TBs yield then decreased when the ultrasonic power was further up from 720W. Consequently, ultrasonic power in the range of 590–850 W was fitted mostly for the highest TBs. As shown in Fig. 2C, the TBs yield was elevated as the ultrasonic time elevated from 2 to 26 min, but the raise of the ultrasonic time did not provide a higher TBs yield. Hence, the most fitted ultrasonic time was in the range of 18–34 min to obtain the highest TBs. Similar to other factors, the water content in ChCl/MA also significantly influenced TBs yield, where an raise of the water content in ChCl/MA from 10 to 30% heightened the TBs yield (Fig. 2D). Howbeit, further raise of the water content in ChCl/MA did not good for the extraction of TBs as the yield dropped. Thus, the water content in ChCl/MA with 20–40% was recommended for the highest TBs.

3.2.2. Results of the BBD

Based on the above single-factor experiment results, the solid to liquid ratio, water content in ChCl/MA, ultrasonic power, and ultrasonic time were then tested by BBD to obtain the optimal UAE-DES conditions

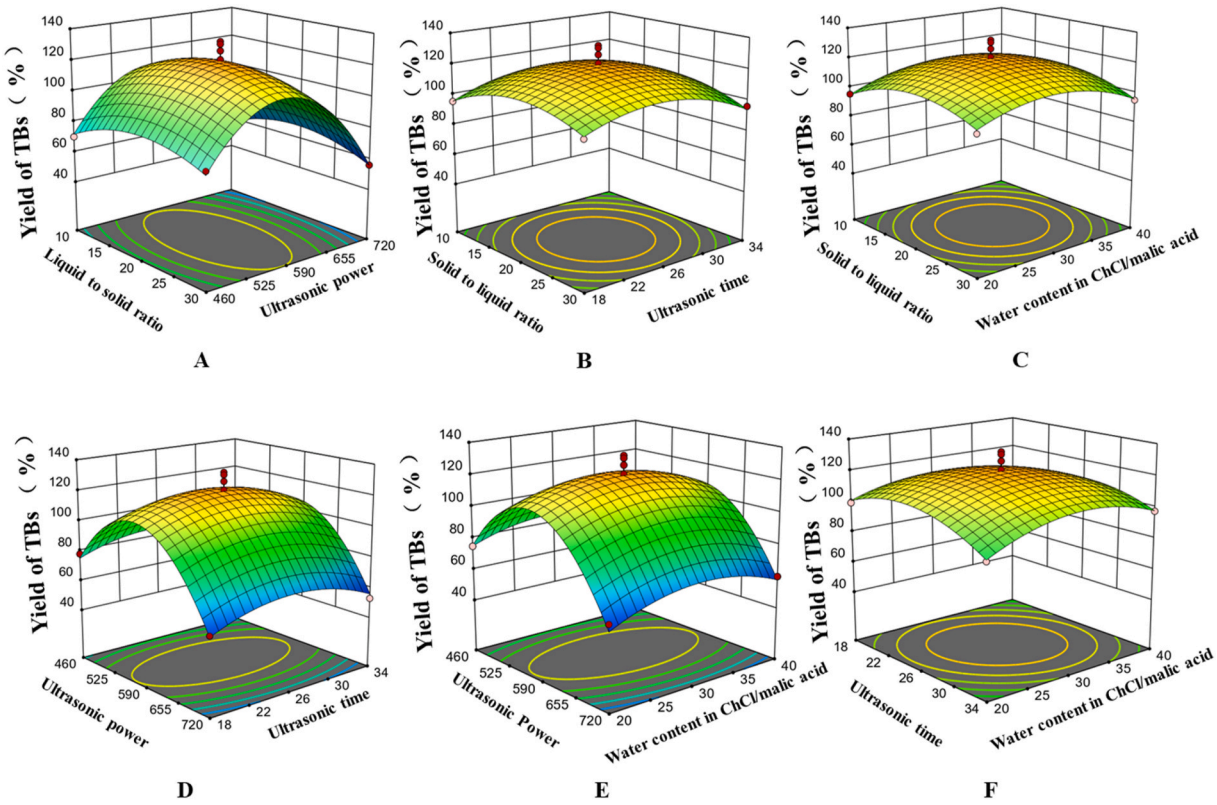

Fig. 3. Response surface analysis of the yield of TBs from the Kangzhuan dark tea powder. (A) the interaction between liquid to solid ratio and ultrasonic power; (B) the interaction between liquid to solid ratio and ultrasonic time; (C) the interaction between liquid to solid ratio and water content in ChCl/MA (%); (D) the interaction between ultrasonic power and ultrasonic time; (E) the interaction between ultrasonic power and water content in ChCl/MA; (F) the interaction between ultrasonic time and water content in ChCl/MA.

with a maximum TBs yield from the KZDT. The BBD design is shown in Table S2. The data for the TBs yield and the coefficients and *p*-values are listed in Table S3. The final model equation of the maximum TBs yield is given as below:

$$Y = +121.13 + 0.5918\,X_1 - 8.44\,X_2 - 1.29\,X_3 - 0.0712\,X_4 - 1.59X1\,X_2 - 1.48\,X1\,X_3 - 1.25 \times 1\,X_4 + 1.15X2\,X_3 + 1.91X2\,X_3 + 3.64X3X_4 - 11.83\,X_1^{\wedge 2} - 43.84\,X_2^{\wedge 2} - 12.93\,X_3^{\wedge 2} - 12.71\,X_4^{\wedge 2}$$

Where, Y is the TBs yield, X_1 *is* the liquid to solid, X_2 *is* the ultrasonic power, X_3 *is* the ultrasonic time, and X_4 *is* the water content in ChCl/MA.

The results indicated that the predicted TBs value of 12.16% KZDT powder could be obtained under the optimal UAE-DES conditions as follows: liquid to solid ratio of 20.37:1 (v/w), ultrasonic power of 577.26 W, ultrasonic time of 25.53 min, and water content of 29.80%. For practical purposes, the optimal UAE-DES conditions were predicted as follows: liquid to solid ratio of 20:1 (v/w), ultrasonic power of 577 W, ultrasonic time of 25 min, and water content of 30%.

ANOVA was applied to analyze the model equation significance, which is shown in Table S4. The *p*-value (<0.0001) indicated that the quadratic model was significant. The coefficient of determination (R^2 = 0.9123) indicated that the predicted results met well with the experimental results. The difference between the predicted determination coefficient (R^2 pre = 0.8374) and R^2 was <0.2. The adjusted coefficient of determination (R^2 Adj = 0.8246) was commensurate to R^2, indicating the predicted and observed values have a strong correlation. The "Lack of Fit F-value" was 0.033 ($p > 0.05$), which indicated the model was effective. The coefficient of variation value (C.V. = 11.10%) suggested the experimental values have a high reliability and precision. Consequently, we concluded that the regression model was reasonable.

As shown in Table S4, the effect of ultrasonic power ($p < 0.0001$) on TBs yield > ultrasonic time ($p = 0.0044$) > the water content in ChCl/MA > liquid to solid ratio ($p = 0.0078$). The response surface plots are shown in Fig. 3 to clarify the interactive effects of four factors on the TBs yield. The interactive effect between the liquid to solid ratio and ultrasonic power (Fig. 3A), ultrasonic power and water content in ChCl/MA (Fig. 3E), were obvious on the TBs yield. The interactive effect between the liquid to solid ratio and ultrasonic time (Fig. 3B), liquid to solid ratio and water content in ChCl/MA (Fig. 3C), ultrasonic power and the ultrasonic time (Fig. 3D), water content in ChCl/MA and ultrasonic time (Fig. 3F), were not significant for the TBs yield.

3.2.3. *Model verification*

The RSM result was verified to corroborate the suitability of this model. The actual max TBs yield (12.59% KZDT powder) was commonly met well with the predicted results (12.16% KZDT powder) under the optimal UAE-DES conditions as follows: water content in ChCl/MA of 30%, liquid to solid ratio of 20:1 mL/g, ultrasonic power of 577 W, and ultrasonic time of 25 min. So, the model was suitable for the extraction of TBs from KZDT. The actual maximal TBs yield was about 11.29% higher than that obtained by UAE-ethanol, suggesting DES has better extraction ability than ethanol. Besides, the TBs yield obtained by ME was 22.68% lower than the TBs value obtained by UAE-DES. Obviously, the application of UAE-DES provided an efficient and green extraction of plant bioactive compounds than UAE-ethanol and ME (Cai et al., 2019; Luo et al., 2020). In a previous study, 29.3% TBs of the instant dark tea could be achieved via submerged fermentation using *Aspergillus niger* (Wang et al., 2017). However, the cost of fermentation is too great for industrial use of TBs, hindering the industrialization of TBs. In addition, lower intermolecular interaction energy, larger accessible solvent surface area, and more hydrogen bonds between ChCl/MA and extracts explain for the efficient extraction ability of ChCl/MA (Fu et al., 2022). Therefore, the customized DES is an efficient and green alternative to

Table 1
Identification of the main chemical profile of TBFs by LC-MS/MS.

NO.	RT [min]	m/z	MW	Formula	Identification	Classification	TBFs	Area (Max.)	Reference Ion
1	1.12	112.0508	111.04354	C4H5N3O	Cytosine	Nucleotides and their derivatives	TBFs2, TBFs3, TBFs4	9.42E+07	[M+H]+1
2	5.07	114.0916	113.08436	C6H11NO	Caprolactam	Others	TBFs3, TBFs4	4.85E+08	[M+H]+1
3	1.52	115.0025	116.00981	C4H4O4	Fumaric acid	Phenolic acids	TBFs1, TBFs2, TBFs3	3.39E+08	[M-H]-1
4	1.45	128.0343	129.04152	C5H7NO3	4-Oxoproline	Amino acids and their derivatives	TBFs1, TBFs2, TBFs3, TBFs4	1.09E+08	[M-H]-1
5	1.45	130.05	129.04268	C5H7NO3	D-(+)-Pyroglutamic acid	Phenolic acids	TBFs1, TBFs2	6.86E+07	[M+H]+1
6	1.11	136.0618	135.05453	C5H5N5	Adenine	Nucleotides and their derivatives	TBFs1, TBFs2, TBFs3, TBFs4, TBFs5	3.34E+08	[M+H]+1
7	0.06	141.1135	140.10621	C6H12N4	Methenamine	Others	TBFs1, TBFs2, TBFs3, TBFs4, TBFs5	1.13E+08	[M+H]+1
8	2.23	152.0567	151.04947	C5H5N5O	Guanine	Nucleotides and their derivatives	TBFs3, TBFs4	1.12E+08	[M+H]+1
9	2.20	169.0134	170.02055	C7H6O5	Gallic acid	Phenolic acids	TBFs1, TBFs2, TBFs3, TBFs4, TBFs5	5.65E+08	[M-H]-1
10	4.25	181.0719	180.06466	C7H8N4O2	Theobromine	Alkaloids	TBFs1, TBFs2	7.44E+07	[M+H]+1
11	4.30	185.042	184.03474	[C5H15NO4P]+	Phosphocholine	Alkaloids	TBFs1, TBFs2, TBFs3, TBFs4	7.73E+08	[M+H]+1
12	0.93	191.0555	192.06276	C7H12O6	D-(−)-Quinic acid	Phenolic acids	TBFs1, TBFs2, TBFs3, TBFs4, TBFs6	4.08E+08	[M-H]-1
13	4.44	192.1383	191.13097	C12H17NO	Diethyltoluamide	Others	TBFs1,TBFs3, TBFs5, TBFs6	3.42E+08	[M+H]+1
14	3.83	192.1383	191.13103	C12H17NO	Diethyl-2-phenylacetamide	Others	TBFs1, TBFs3, TBFs4, TBFs5	2.71E+08	[M+H]+1
15	6.60	195.0876	194.0803	C8H10N4O2	Caffeine	Alkaloids	TBFs1, TBFs2, TBFs3, TBFs4, TBFs5	6.90E+09	[M+H]+1
16	6.96	199.0576	176.06838	C7H12O5	2-Isopropylmalic acid	Phenolic acids	TBFs1	9.61E+08	[M+Na]+1
17	35.48	204.1383	203.13102	C13H17NO	Crotamiton	Amino acids and their derivatives	TBFs1, TBFs2, TBFs3, TBFs4, TBFs5, TBFs6	1.12E+08	[M+H]+1
18	33.78	210.0769	211.08414	C11H9N5	1-Phenyl-1H-pyrazolo[3,4-d] pyrimidin-4-amine	Others	TBFs1	1.69E+07	[M-H]-1
19	33.59	214.2529	213.24559	C14H31N	1-Tetradecylamine	Others	TBFs1, TBFs2, TBFs3, TBFs4, TBFs5, TBFs6	4.44E+08	[M+H]+1
20	4.54	217.1046	216.09734	C11H12N4O	6-(4-methoxyphenyl) pyrimidine-2,4-diamine	Others	TBFs1, TBFs2, TBFs5	5.42E+08	[M+H]+1
21	35.72	221.1545	222.16182	C14H22O2	2,5-di-tert-Butylhydroquinone	Anthraquinones	TBFs1, TBFs2, TBFs3, TBFs4, TBFs5, TBFs6	2.51E+07	[M-H]-1
22	35.56	233.1547	234.16195	C15H24O3	Ilicic Acid	Others	TBFs1, TBFs2, TBFs3, TBFs4, TBFs5, TBFs6	4.45E+07	[M-H]-1
23	35.34	239.0674	240.0747	C10H12N2O5	Dinoterb	Others	TBFs1, TBFs2, TBFs3, TBFs4, TBFs5, TBFs6	2.75E+07	[M-H]-1
14	5.31	239.1488	238.14146	C10H22O6	Pentaethylene glycol	Others	TBFs1, TBFs2, TBFs3, TBFs4, TBFs5, TBFs6	7.11E+09	[M+H]+1
25	33.64	256.2996	255.29236	C17H37N	N-Methyldioctylamine	Others	TBFs1, TBFs2, TBFs3, TBFs4, TBFs5, TBFs6	1.04E+08	[M+H]+1
26	35.96	265.1482	266.15552	C12H26O4S	(Dodecyloxy) sulfonic acid	Phenolic acids	TBFs1, TBFs2, TBFs3, TBFs4, TBFs5, TBFs6	4.13E+08	[M-H]-1
27	1.85	268.1039	267.09658	C10H13N5O4	2′-Deoxyguanosine	Nucleotides and their derivatives	TBFs1, TBFs2, TBFs3, TBFs4	2.68E+08	[M+H]+1
28	1.21	273.0215	274.21424	C14H9ClN2S	(−)-Epiafzelechin	Flavonoids	TBFs1	8.93E+07	[M-H]-1
29	35.27	277.1449	278.15215	C16H22O4	Alpha-Linolenic acid	Lipids	TBFs1, TBFs2, TBFs3, TBFs4, TBFs5, TBFs6	6.32E+07	[M-H]-1
30	36.26	279.1589	278.15182	C16H22O4	Gamma-Linolenic acid	Lipids	TBFs1, TBFs2, TBFs3, TBFs4, TBFs5, TBFs6	2.44E+08	[M+H]+1
31	6.21	283.1749	282.16758	C17H14O4	3,5-Dimethoxyflavone	Flavonoids	TBFs1, TBFs2, TBFs3, TBFs4, TBFs5, TBFs6	6.79E+09	[M+H]+1

(*continued on next page*)

Table 1 (*continued*)

NO.	RT [min]	m/z	MW	Formula	Identification	Classification	TBFs	Area (Max.)	Reference Ion
32	40.16	284.2945	283.28722	C10H13N5O5	Guanosine	Nucleotides and their derivatives	TBFs1	5.57E+08	[M+H]+1
33	35.56	284.3309	283.32365	C10H13N5O5	Isoguanosine	Nucleotides and their derivatives	TBFs1, TBFs2, TBFs3, TBFs4, TBFs5, TBFs6	2.66E+08	[M+H]+1
34	40.21	293.1796	294.18687	C17H14N2O3	Cyclopenin	Others	TBFs1	2.66E+08	[M-H]-1
35	28.94	301.0721	302.07942	C15H10O7	Quercetin	Flavonoids	TBFs3	4.37E+07	[M-H]-1
36	20.35	303.0862	302.07882	C16H14O6	Hesperetin	Flavonoids	TBFs1, TBFs2	3.30E+08	[M+H]+1
37	40.70	325.1846	326.19191	C18H30O3S	4-Dodecylbenzenesulfonic acid	Organic acid	TBFs1	2.11E+08	[M-H]-1
38	42.48	338.3416	337.33428	C22H43NO	Erucamide	Derivatives of unsaturated fatty acids	TBFs1, TBFs2, TBFs3, TBFs4, TBFs5, TBFs6	4.16E+09	[M+H]+1
39	38.01	339.2331	340.24037	C15H16O9	6,7-Dihydroxycoumarin-6-glucoside	Flavonoids	TBFs1	2.90E+09	[M-H]-1
40	32.62	343.1175	342.11012	C19H18O6	Zapotin	Flavonoids	TBFs1, TBFs4	1.11E+08	[M+H]+1
41	36.24	383.2039	360.21464	C22H26N2O4	Tofisopam	Others	TBFs1, TBFs2, TBFs3, TBFs4, TBFs5, TBFs6	1.41E+08	[M+Na]+1
42	37.01	425.2144	402.22518	C24H31FO4	Citroflex A-4	Others	TBFs1, TBFs2, TBFs3, TBFs4, TBFs5, TBFs6	3.59E+08	[M+Na]+1
43	11.26	476.3063	475.6 43	C23H42NO7P	LysoPE(0:0/18:3(6Z,9Z,12Z))	Lipids	TBFs1, TBFs2, TBFs3, TBFs4, TBFs5, TBFs6	1.29E+10	[M+H]+1
44	12.95	520.3327	520.29883	C22H46O12	Gallocatechin gallate derivative	Flavonoids derivatives	TBFs1, TBFs2, TBFs3, TBFs4, TBFs5, TBFs6	8.86E+09	[M+H]+1
45	14.66	564.3588	564.32499	C26H28O14	Apigenin 6-C-glucoside 8-C-arabinoside	Flavonoids	TBFs1, TBFs2, TBFs3, TBFs4, TBFs5, TBFs6	5.42E+09	[M+H]+1
46	18.19	579.1731	580.17975	C27H32O14	Naringin	Flavonoids	TBFs1	5.71E+07	[M-H]-1
47	20.36	609.1837	610.1904	C28H34O15	Neohesperidin	Flavonoids	TBFs1, TBFs2, TBFs3, TBFs4, TBFs5	1.30E+09	[M-H]-1
48	16.35	613.3401	590.35125	C26H54O14	PEG n13	Others	TBFs2, TBFs4, TBFs5, TBFs6	4.69E+07	[M+Na]+1
49	17.94	652.4113	651.40398	C28H58O15	PEG n14	Others,	TBFs1, TBFs2, TBFs3, TBFs4, TBFs5, TBFs6	7.90E+08	[M+H]+1

Note: All the chemicals were screened by the following criteria: mzCloud Best Match is equal or greater than to 85, Area (Max.) is equal or greater than to 10^5.

extracting TBs from dark tea.

3.3. Characterization of the chemical components in the TBFs

3.3.1. Full mass spectrometric analysis

It has been reported that TBs contain a large amount of complex heterogeneous components, such as phenolics, flavonoids, lipids, proteins, carbohydrates, and amino acids (Gong et al., 2012; Kuang et al., 2020; Xiao et al., 2020). However, few studies have elucidated its chemical composition. Here, TBs were fractionated and separated into six TBFs, namely, TBFs1, TBFs2, TBFs3, TBFs4, TBFs5, and TBFs6. Chemical components in all TBFs were identified using LC-MS/MS analysis. As shown in Table 1, 49 chemicals with mzCloud Best Match ≥85 and Area (Max.) ≥ 10^5 were screened from TBFs under both positive and negative ion modes. These included 10 flavonoids, 6 phenolic acids, 6 nucleotides and derivatives, 3 alkaloids, 3 lipids, 2 amino acids, 1 terpene, and other metabolites. Notably, the Area (Max.) values of LysoPE (0:0/18:3(6Z,9Z,12Z)) (m/z 476.31), gallocatechin gallate derivative (m/z 520.33), caffeine (m/z 195.09), 3,5-dimethoxyflavone (m/z 283.17), apigenin 6-C-glucoside 8-C-arabinoside (m/z 564.36), 6,7-dihydroxycoumarin-6-glucoside (m/z 339.23), erucamide (m/z 338.34), and neohesperidin (m/z 609.18) were equal or greater than 10^9, which indicated that these compounds are the leading compounds of TFBs. The LC-MS/MS spectra for 6,7-dihydroxycoumarin-6--glucoside, erucamide, caffeine, and neohesperidin are shown in Fig. 4. LysoPE (0:0/18:3(6Z,9Z,12Z)) and caffeine were reported in Tibetan tea (Liu Y.T. et al., 2022). In addition, as shown in Table 1, the 49 chemicals had different distributions in six TBFs. Naringin (m/z 579.17), 6, 7-dihydroxycoumarin-6-glucoside (m/z 339.23), 4-dodecylbenzenesulfonic acid (m/z 325.18), cyclopenin (m/z 293.18), guanosine (m/z 284.29), 1-phenyl-1h-pyrazolo[3,4-d]pyrimidin-4-amine (m/z 210.08), (−)-epiafzelechin (m/z 273.02), and 2-isopropylmalic acid (m/z 199.06) were identified only in TBFs1. D-(+)-pyroglutamic acid (m/z 130.05), theobromine (m/z 181.07), and hesperetin (m/z 303.09) were identified only in TBFs1 and TBFs2. Of all the compounds, naringin is a flavanone glycoside that is found in the Chinese herbal medicines and citrus plants, with numerous biological and pharmacological properties (Chen et al., 2016). (−)-Epiafzelechin is a flavan-3-ol commonly found in plants with anti-inflammatory, antioxidant, and bone-protective effects (Wong et al., 2014). 2-Isopropylmalic acid is an organic acid discovered in wines (Ricciutelli et al., 2020). Zapotin (m/z 343.12), a polymethoxyflavone with potential therapeutic attributes mainly in citrus plants (Strawa et al., 2021), was identified only in TBFs1 and TBFs4. The conclusion we can draw from the above results is that some compounds were only found in specific fractions. The reason is that the separation elution of TBs was performed while progressively increasing the polarity of the mobile phase (methanol: water), indicating compounds with different polarities were resolved in the mobile phase of different polarity (Yang et al., 2019). Therefore, a solid-phase separation procedure with silica gel as the stationary phase and 100−0% methanol aqueous solutions as the mobile phase was first provided as a convenient and cost-effective strategy to separate more compounds from TBs.

3.4. Principal component analysis

To further investigate the difference in chemical composition

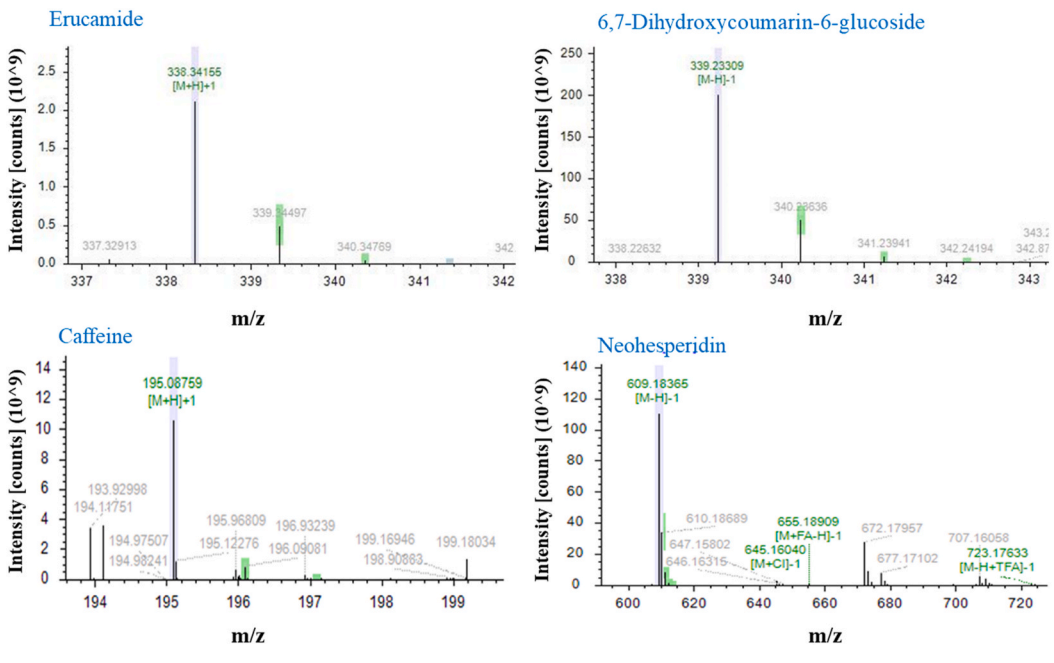

(A)

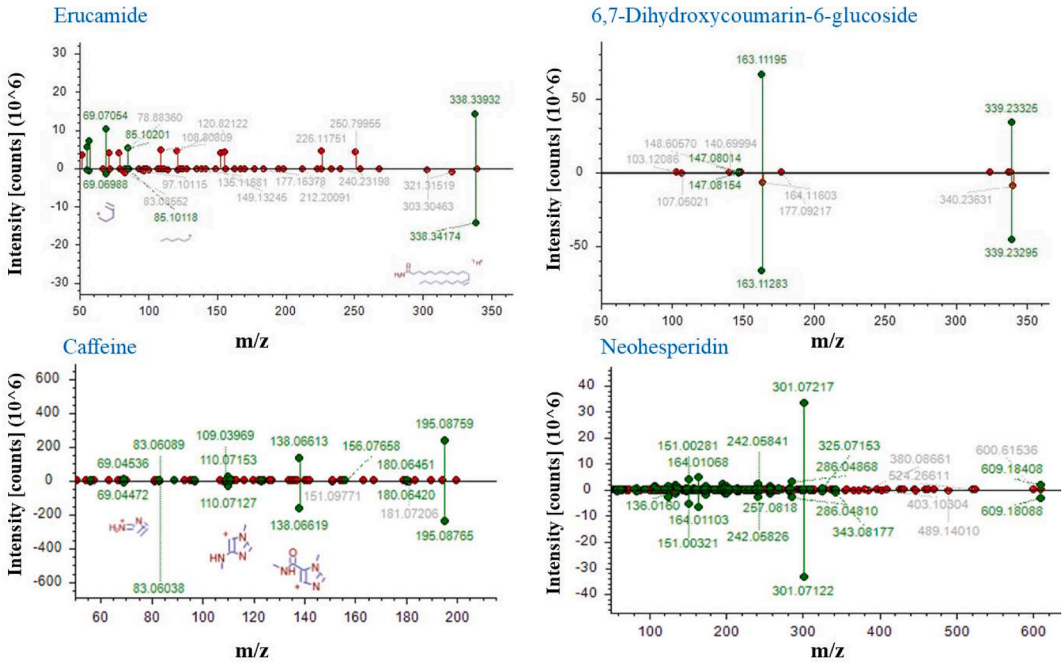

(B)

Fig. 4. Mass spectra of 4 leading compounds in TBFs. (A) The mother ion ([M-H]-) of each peak; (B) The fragment ions of each peak.

detected among the six TBFs, a principal component analysis (PCA) was performed on LC-MS/MS data. As shown in Fig. 5A, in the PCA of all the LC-MS/MS data, the PC1 and PC2 are 68.9% and 28.4%, respectively, they explained 97.3% of the total variance across all samples. The PCA score plot showed that TBFs3, TBFs4, TBFs5, and TBFs6 were closely clustered in the PCA, and a significant separation was observed between TBFs1 and TBFs2, indicating that the chemical composition of TBFs3, TBFs4, TBFs5, and TBFs6 elution was the closest. A similar result was obtained in Fig. 5B, TBFs1, TBFs2, TBFs3, TBFs4, TBFs5, and TBFs6 can be distinguished as three groups on the hierarchical clustering analysis. Collectively, these results, for the first time, indicated that different chemical compounds in TBs were eluted by silica gel powder combined with different concentrations of methanol solutions.

3.5. Analysis of antioxidant capacities of TBFs

Oxidative stress is considered an important factor leading to aging and disease (Ma et al., 2022). Some studies have proved that dark tea

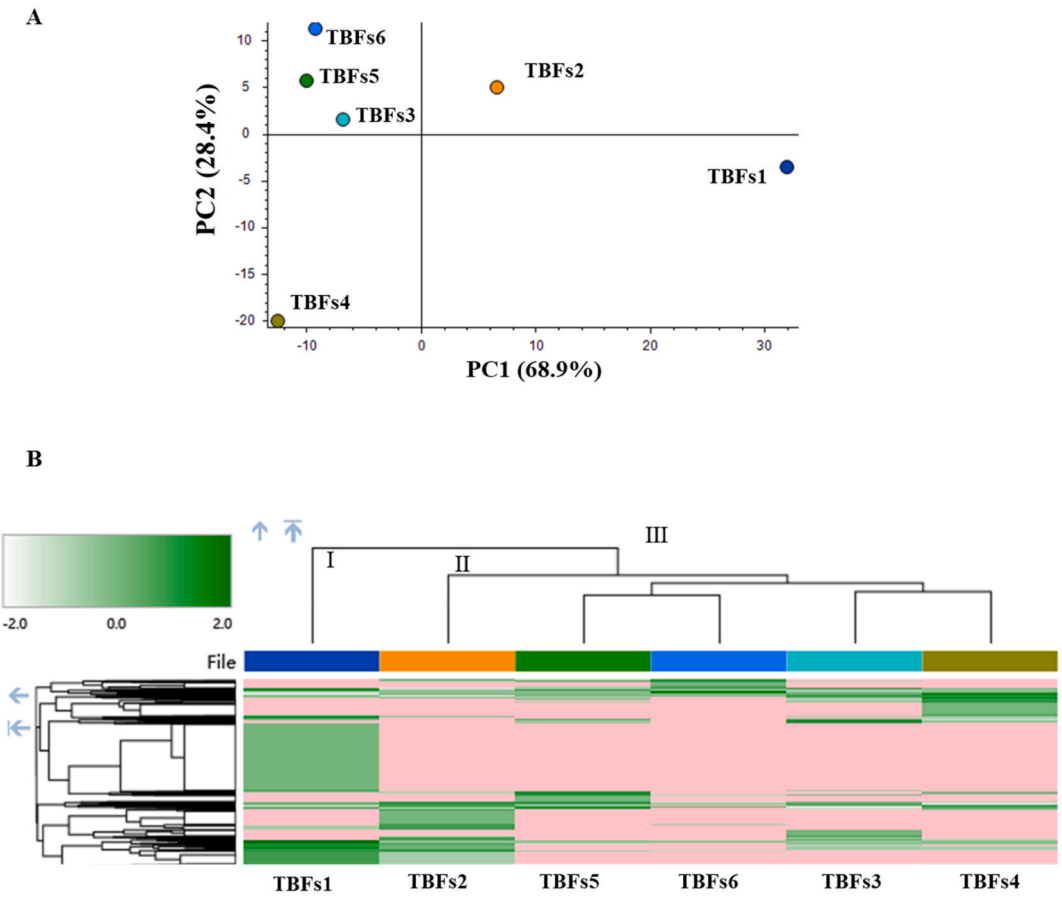

Fig. 5. Principal component analysis and hierarchical cluster analysis of chemical components in TBFs.

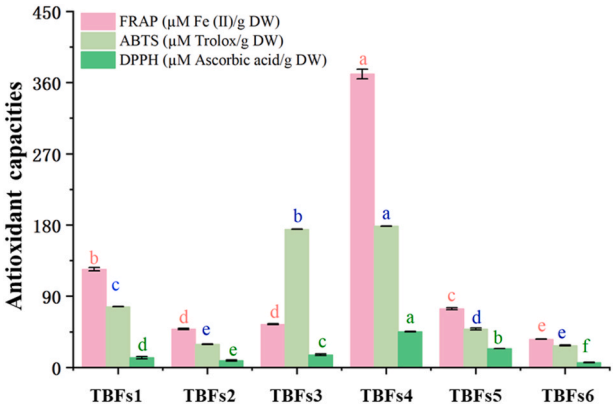

Fig. 6. DPPH free radical scavenging, ABTS free radical scavenging, and FRAP effect of TBFs. Values with superscript letters (a–f) in black, blue, and green colors respectively represent significant differences ($p < 0.05$) in FRAP, ABTS, and DPPH values across groups. (For interpretation of the references to color in this figure legend, the reader is referred to the Web version of this article.)

exhibited strong antioxidant activity (Lin et al., 2021). It is widely known that TBs are crucial for the antioxidant activity of dark teas. To compare the *in vitro* antioxidant activities of all TBFs, DPPH free radical scavenging, ABTS free radical scavenging, and FRAP assay were carried.

The results are shown in Fig. 6. Generally, the antioxidant capacities of six TBFs were verified by the DPPH radical scavenging assay in the order of TBFs4 > TBFs5> TBF3 > TBFs1 > TBFs2>TBFs6. The antioxidant capacities of six TBFs were verified by the ABTS free radical scavenging assay in the order of TBFs4 > TBFs3> TBF2 > TBFs5 > TBFs2 = TBFs6. The antioxidant capacities of six TBFs were also verified by the FRAP assay in the order of TBFs4 > TBFs1> TBF5 > TBF3 = TBFs2 > TBFs6. As the results of DPPH, ABTS, and FRAP, the TBFs4 showed the highest antioxidant activity among all the TBFs, indicating that 60−40% methanol aqueous solution is most suitable for the elution of antioxidants in TBs. Meanwhile, the DPPH, ABTS, and FRAP values of TBFs4 were 45.08 ± 0.42 μM Ascorbic acid/g DW, 178.52 ± 0.29 μM Trolox/g DW, and 370.85 ± 6.00 μM Fe(II)/g DW, respectively. This result indicated that the TBFs from Tibetan tea had different DPPH free radical scavenging, ABTS free radical scavenging, and FRAP effects, which was accordant with the conclusion of a prior study, which reported that extracts from Tibetan tea had strong DPPH and ABTS radical scavenging capacities (Liu Y.T. et al., 2022).

4. Conclusions

This study developed a UAE-DES based extraction method to produce TBs from KZDT, and revealed the chemical composition of TFBs eluded by silica gel from TBs using LC-MS/MS. Under the optimal conditions of UAE-ChCl/MA, the highest yield (12.59%) of TBs from KZDT was achieved. A total of 49 chemicals were identified in TFBs, and 6,7-dihydroxycoumarin-6-glucoside, erucamide, caffeine, and neohesperidin were among the leading compounds in the TBFs. Results from *in vitro* antioxidant capacity showed that all TBFs exhibited antioxidant activities, while TBFs4 displayed the highest antioxidant activity. Consequently, it is necessary to further clarify specific antioxidants in TBs and delve into the antioxidant activity of TBs using *in vivo* models in the future. Overall, our findings not only furnish a theoretical basis for the extraction of KZDT with high TBs, but also provide a reference to understand the chemical composition of TBs in KZDT. These results have the potential to guide the further development of KZDT products.

CRediT authorship contribution statement

Yi Liu: conceived the project, performed the experiments, nalyzed the data and wrote the draft. **Hong-Yan Liu:** analyzed the data and wrote the draft, revised and edited the manuscript. **Xiao Yang:** revised and edited the manuscript. **Fan Zhu:** revised and edited the manuscript. **Ding-Tao Wu:** revised and edited the manuscript. **Hua-Bin Li:** revised and edited the manuscript. **Ren-You Gan:** conceived the project, revised and edited the manuscript, provided funding support, The final version was approved by all authors.

Declaration of competing interest

The authors declare that they have no known competing financial interests or personal relationships that could have appeared to influence the work reported in this paper.

Acknowledgments

This work was supported by the Local Financial Funds of National Agricultural Science and Technology Center, Chengdu (NASC2021TD01; NASC2021KR08), Natural Science Foundation of China (32202169), The Agricultural Science and Technology Innovation Program (ASTIP- IUA-2022002), and Sichuan Science and Technology Plan Seedling Project (2021JDRC0141).

Appendix A. Supplementary data

Supplementary data to this article can be found online at https://doi.org/10.1016/j.crfs.2022.10.019.

References

Benvenutti, L., Zielinski, A.A.F., Ferreira, S.R.S., 2022. Pressurized aqueous solutions of deep eutectic solvent (DES): a green emergent extraction of anthocyanins from a Brazilian berry processing by-product. Food Chem. X 13, 100236. https://doi.org/10.1016/j.fochx.2022.100236.

Cai, C., Yu, W., Wang, C., Liu, L., Li, F., Tan, Z., 2019. Green extraction of cannabidiol from industrial hemp (*Cannabis sativa* L.) using deep eutectic solvents coupled with further enrichment and recovery by macroporous resin. J. Mol. Liq. 287, 110957 https://doi.org/10.1016/j.molliq.2019.110957.

Chen, R., Qi, Q.L., Wang, M.T., Li, Q.Y., 2016. Therapeutic potential of naringin: an overview. Pharm. Biol. 54 (12), 3203–3210. https://doi.org/10.1080/13880209.2016.1216131.

Chen, X., Hu, Y., Wang, B., Chen, Y., Yuan, Y., Zhou, W., Song, W., Wu, Z., Li, X., 2022. Characterization of theabrownins prepared from tea polyphenols by enzymatic and chemical oxidation and their inhibitory effect on colon cancer cells. Front. Nutr. 9 (3), 1–13. https://doi.org/10.3389/fnut.2022.849728.

Ding, J., Mei, S., Gao, L., Wang, Q., Ma, H., Chen, X., 2022. Tea processing steps affect chemical compositions, enzyme activities, and antioxidant and anti-inflammatory activities of coffee leaves. Food Front. https://doi.org/10.1002/fft2.136.

Durak, A., Gawlik-Dziki, U., 2014. The study of interactions between active compounds of coffee and willow (*Salix* sp.) bark water extract. BioMed Res. Int. 2014, 386953 https://doi.org/10.1155/2014/386953.

Fu, X., Belwal, T., He, Y., Xu, Y., Li, L., Luo, Z., 2022. UPLC-Triple-TOF/MS characterization of phenolic constituents and the influence of natural deep eutectic solvents on extraction of *Carya cathayensis Sarg.* peels: composition, extraction mechanism and *in vitro* biological activities. Food Chem. 15 (370), 131042 https://doi.org/10.1016/j.foodchem.2021.131042.

Gan, R.Y., Wang, M.F., Lui, W.Y., Wu, K., Dai, S.H., Sui, Z.Q., Corke, H., 2017. Diversity in antioxidant capacity, phenolic contents, and flavonoid contents of 42 edible beans from China. Cereal Chem. 94 (2), 291–297. https://doi.org/10.1094/CCHEM-03-16-0061-R.

Gong, J.S., Tang, C., Peng, C.X., 2012. Characterization of the chemical differences between solvent extracts from Pu-erh tea and Dian Hong black tea by CP-Py-GC/MS. J. Anal. Appl. Pyrolysis. 95, 189–197. https://doi.org/10.1016/j.jaap.2012.02.006.

Huang, F., Zheng, X., Ma, X., Jiang, R., Zhou, W., Zhou, S., Zhang, Y., Lei, S., Wang, S., Kuang, J., Han, X., Wei, M., You, Y., Li, M., Li, Y., Liang, D., Liu, J., Chen, T., Yan, C., Jia, W., 2019. Theabrownin from Pu-erh tea attenuates hypercholesterolemia via modulation of gut microbiota and bile acid metabolism. Nat. Commun. 10 (1), 4971. https://doi.org/10.1038/s41467-019-12896-x.

Jin, W., Zhou, L., Yan, B., Yan, L., Liu, F., Tong, P., Yu, W., Dong, X., Xie, L., Zhang, J., Xu, Y., Li, C., Yuan, Q., Shan, L., Efferth, T., 2018. Theabrownin triggers DNA damage to suppress human osteosarcoma U2OS cells by activating p53 signalling pathway. J. Cell Mol. Med. 22 (9), 4423–4436. https://doi.org/10.1111/jcmm.13742.

Kuang, J., Zheng, X., Huang, F., Wang, S., Li, M., Zhao, M., Sang, C., Ge, K., Li, Y., Li, J., Rajani, C., Ma, X., Zhou, S., Zhao, A., Jia, W., 2020. Anti-adipogenic effect of theabrownin is mediated by bile acid alternative synthesis via gut microbiota remodeling. Metabolites 10 (11), 1–16. https://doi.org/10.3390/metabo10110475.

Lin, F.J., Wei, X.L., Liu, H.Y., Li, H., Xia, Y., Wu, D.T., Zhang, P.Z., Gandhi, G.R., Hua-Bin, Li, Gan, R.Y., 2021. State-of-the-art review of dark tea: from chemistry to health benefits. Trends Food Sci. Technol. 109, 126–138. https://doi.org/10.1016/j.tifs.2021.01.030.

Liu, Y.T., Huang, W., Zhang, C., Li, C., Fang, Z., Zeng, Z., Hu, B., Chen, H., Wu, W., Wang, T., Lan, X., 2022. Targeted and untargeted metabolomic analyses and biological activity of Tibetan tea. Food Chem. 384, 132517 https://doi.org/10.1016/j.foodchem.2022.132517.

Liu, Yi, Kong, K.W., Wu, D.T., Liu, H.Y., Li, H.B., Zhang, J.R., Gan, R.Y., 2022a. Pomegranate peel-derived punicalagin: ultrasonic-assisted extraction, purification, and its α-glucosidase inhibitory mechanism. Food Chem. 374, 1–10. https://doi.org/10.1016/j.foodchem.2021.131635.

Liu, Yi, Liu, H.Y., Li, S.H., Ma, W., Wu, D.T., Li, H., Bin Xiao, A.P., Liu, L.L., Zhu, F., Gan, R.Y., 2022b. *Cannabis sativa* bioactive compounds and their extraction, separation, purification, and identification technologies: an updated review. Trends Anal. Chem. 149, 116554 https://doi.org/10.1016/j.trac.2022.116554.

Liu, Yi, Liu, H.Y., Xia, Y., Guo, H., He, X.Q., Li, H., Wu, D.T., Geng, F., Lin, F.J., Li, H.B., Zhuang, Q.G., Gan, R.Y., 2021. Screening and process optimization of ultrasound-assisted extraction of main antioxidants from sweet tea (*Lithocarpus litseifolius* [Hance] Chun). Food Biosci. 43, 101277 https://doi.org/10.1016/j.fbio.2021.101277.

Luo, Q., Zhang, J.R., Li, H.B., Wu, D.T., Geng, F., Corke, H., Wei, X.L., Gan, R.Y., 2020. Green extraction of antioxidant polyphenols from green tea (*Camellia sinensis*). Antioxidants 9 (9), 1–15. https://doi.org/10.3390/antiox9090785.

Ma, W., Shi, Y., Yang, G., Shi, J., Ji, J., Zhang, Y., Wang, J., Peng, Q., Lin, Z., Lv, H., 2022. Hypolipidaemic and antioxidant effects of various Chinese dark tea extracts obtained from the same raw material and their main chemical components. Food Chem. 375, 131877 https://doi.org/10.1016/j.foodchem.2021.131877.

Mai, Y.H., Zhuang, Q.G., Li, Q.H., Du, K., Wu, D.T., Li, H.B., Xia, Y., Zhu, F., Gan, R.Y., 2022. Ultrasound-assisted extraction, identification, and quantification of antioxidants from 'Jinfeng' Kiwifruit. Foods 11 (6), 827. https://doi.org/10.3390/foods11060827.

Ricciutelli, M., Bartolucci, G., Campana, R., Salucci, S., Benedetti, S., Caprioli, G., Maggi, F., Sagratini, G., Vittori, S., Lucarini, S., 2020. Quantification of 2- and 3-isopropylmalic acids in forty Italian wines by UHPLC-MS/MS triple quadrupole and evaluation of their antimicrobial, antioxidant activities and biocompatibility. Food Chem. 321, 126726 https://doi.org/10.1016/j.foodchem.2020.126726.

Strawa, J.W., Jakimiuk, K., Tomczyk, M., 2021. Zapotin, a polymethoxyflavone, with potential therapeutic attributes. Int. J. Mol. Sci. 22 (24), 13227 https://doi.org/10.3390/ijms222413227.

Wang, C.K., Yang, H.L., Li, J.Y., 2021. Combination of microwave, ultrasonic, enzyme assisted method for curcumin species extraction from turmeric (*Curcuma Longa* L.) and evaluation of their antioxidant activity. eFood 2 (2), 73–80. https://doi.org/10.2991/efood.k.210329.001.

Wang, Q., Belščak-Cvitanović, A., Durgo, K., Chisti, Y., Gong, J., Sirisansaneeyakul, S., Komes, D., 2018. Physicochemical properties and biological activities of a high-theabrownins instant Pu-erh tea produced using *Aspergillus tubingensis*. LWT–Food Sci. Technol. 90, 598–605. https://doi.org/10.1016/j.lwt.2018.01.021.

Wang, Y., Zhang, M., Zhang, Z., Lu, H., Gao, X., Yue, P., 2017. High-theabrownins instant dark tea product by *Aspergillus niger* via submerged fermentation: α-glucosidase and pancreatic lipase inhibition and antioxidant activity. J. Sci. Food Agric. 97 (15), 5100–5106. https://doi.org/10.1002/jsfa.8387.

Wong, K.C., Law, M.C., Wong, M.S., Chan, T.H., 2014. Development of a UPLC-MS/MS bioanalytical method for the pharmacokinetic study of (-)-epiafzelechin, a flavan-3-ol with osteoprotective activity, in C57BL/6J mice. J. Chromatogr., B: Anal. Technol. Biomed. Life Sci. 967, 162–167. https://doi.org/10.1016/j.jchromb.2014.07.028.

Wu, E., Zhang, T., Tan, C., Peng, C., Chisti, Y., Wang, Q., Gong, J., 2020. Theabrownin from Pu-erh tea together with swinging exercise synergistically ameliorates obesity and insulin resistance in rats. Eur. J. Nutr. 59 (5), 1937–1950. https://doi.org/10.1007/s00394-019-02044-y.

Xiao, Y., Li, M., Wu, Y., Zhong, K., Gao, H., 2020. Structural characteristics and hypolipidemic activity of theabrownins from dark tea fermented by single species *Eurotium cristatum* PW-1. Biomolecules 10 (2), 204. https://doi.org/10.3390/biom10020204.

Xie, H., Li, X., Ren, Z., Qiu, W., Chen, J., Jiang, Q., Chen, B., Chen, D., 2018. Antioxidant and cytoprotective effects of Tibetan tea and its phenolic components. Molecules 23 (2), 1–13. https://doi.org/10.3390/molecules23020179.

Xie, J., Song, X., Zhang, Y., Zhang, M., Li, X., He, L., 2019. Rapid determination of nosiheptide in feed based on dispersive SPE coupled with HPLC. J. Separ. Sci. 42 (3), 706–715. https://doi.org/10.1002/jssc.201801036.

Yang, Z., Guo, P., Han, R., Wu, D., Gao, J.M., Wu, S., 2019. Methanol linear gradient counter-current chromatography for the separation of natural products: *Sinopodophyllum hexandrum* as samples. J. Chromatogr. A 1603, 251–261. https://doi.org/10.1016/j.chroma.2019.06.055.

Zheng, Q., Li, W., Gao, X., 2021. The effect of storage time on tea polyphenols, catechin compounds, total flavones and the biological activity of Ya'an Tibetan tea (*Camellia sinensis*). J. Food Process. Preserv. 8, 1–11. https://doi.org/10.1111/jfpp.16004.

Zheng, Q., Li, W., Zhang, H., Gao, X., Tan, S., 2020. Optimizing synchronous extraction and antioxidant activity evaluation of polyphenols and polysaccharides from Ya'an Tibetan tea (*Camellia sinensis*). Food Sci. Nutr. 8 (1), 489–499. https://doi.org/10.1002/fsn3.1331.

Zhu, F.M., Li, J.X., Ma, Z.L., Li, J., Du, B., 2021. Structural identification and *in vitro* antioxidant activities of anthocyanins in black chokeberry (*Aronia melanocarpa* lliot). eFood 2 (4), 201–208. https://doi.org/10.2991/assehr.k.211125.004.

Zou, Y., Xu, T., Chen, S., Liu, T., Huang, Y., Science, T., Horticulture, C., 2016. Effect of harvest date and stalk section on selected strength characteristics of *Turkish oregano (Origanum onites l)*. Afr. J. Tradit., Complementary Altern. Med. 13 (4), 191–198. https://doi.org/10.21010/ajtcam.v13i4.25.

Zou, Y.Y., Fan, F.J., Fang, Y., Li, P., Xia, J., Shen, X.C., Liu, Q., Hu, Q.H., 2021. Neuroprotective effect of alkylresorcinols from wheat bran in HT22 cells: correlation with *in vitro* antioxidant activity. eFood 2 (1), 13–20. https://doi.org/10.2991/efood.k.210125.001.